Cumhuriyet Üniversitesi Fen Fakültesi
Fen Bilimleri Dergisi (CFD), Cilt:36, No: 3 Özel Sayı (2015)
ISSN: 1300-1949

Cumhuriyet University Faculty of Science
Science Journal (CSJ), Vol. 36, No: 3 Special Issue (2015)
ISSN: 1300-1949

The Study and Analysis of Neutron Activation with the Application of Gamma Ray Emission

Hamed MORADİ[1,*], Taiyeb NAMDARAN[2], Mohammad Rasool EYVAZİ[3], Iman POURDAD[3]

[1]*Researcher and lecturer at Iran Technical and Vocational Training Organization (TVTO)*

[2]*Researcher and student at Educational Organization*

[3]*Electronics Student*

Received: 01.02.2015; Accepted: 05.05.2015

Abstract. In the neutron activation method, gamma ray is used to trigger and activate neutron. In this method, isotropic neutron sources, its generators, and thermal triggers are studied and analyzed. In this paper, a number of computational and analytical methods, including Monte-Carlo simulation method and Maxwell-Boltzmann method, have been used to enable us to perform large-sample prompt gamma neutron-activation analysis (LS-PGNAA) and to use this large-sample in simulation and laboratory samples.

Keywords: Neutron, density, LS-PGNAA, gamma, atomic mass

1. INTRODUCTION

In this paper, we have made an effort, with the help of simulation and computational methods, to produce a large emission of Gamma ray in order to activate and trigger neutron; therefore, to reach this aim, we have utilized isotropic samples, generators' sources, and a number of practical laboratory and non-intrusive methods to determine neutron density distribution. This would enable us to perform the activation practically.

2. EXPLANATION

When the interaction between neutron and matter takes place, there is a possibility for different sorts of scattering, absorption, and gap to occur. Photoelectric effect is described as the transmission of whole gamma energy to an electron in the inner shell electrons. After the energy absorption, the electron leaves the atom with an energy equal to the incident gamma ray energy minus the electron binding energy. The gap in the inner shells is filled with an electron from the higher shells, and the X-ray and auger electrons are finally radiated, which are due to low energy levels easily absorbed into the matter. As result, they are often not able to escape the matter.

*Corresponding author. *Email address*: *Hamedlee@yahoo.com*

Special Issue: The Second National Conference on Applied Research in Science and Technology

http://dergi.cumhuriyet.edu.tr/cumuscij

Compton scattering is defined as the partial transmission of gamma-ray energy to the electron at the time of collision; when no energy is absorbed, only a part of the energy is transmitted to the detector. The part of the transmitted energy to the electron from the incident gamma ray falls in the continuous Compton, that is approximately in the area between zero and maximum energy. When after the collision, the remainder of the energy, e.g. Compton gamma, are fully absorbed in the detector matter, the Compton electron energy and the absorbed energy or the consecutive absorbed energies are recorded at the maximum energy. The remaining part and the energy variable, which are the result of the part of the Compton distribution in a continuous spectrum and the absorbed collection of other levels of maximum gamma in equal energy, do not provide us with any useful information in the analysis of neutron activation. The maximum Single Escape (SE) and Double Escape (DE) Peak are also advantageous in the analysis of activation in comparison with their discrete values of energy.

In the neutron activation method based on the small-sample prompt gamma emission, the self-shielding of neutrons can be ignored. When the neutron beams are used with the small-samples in the neutron activation method from the prompt gamma, the appropriate temperature is lower than the heat temperature. As a result, more effective neutrons are selected. Since the cross-section is in reverse proportion with the speed of capturing the neutrons, the colder neutrons in component analysis in a sample matter in a constant flux, result in a more effective and detection and higher sensitivity, and in areas distant from neutron source, they result in colder neutrons and gamma with lower energy in the sample area. In the instrumental method of neutron activation, delayed gamma spectrum is recorded in a position other than when a sample is under radiation. Two better positions, therefore, can be selected: one position is when neutron flux is the highest possible, and other position is when background gamma is the lowest possible, and also when the domain of the detector is the largest, that is the measurement domain is not so small that it causes distortion in the spectrum, but it is large enough for the measurement of the minimum detection over a specific period of time. In the prompt gamma neutron activation method, to improve the neutron flux, exposure and measurement positions are the same. The sample can placed close to the reactor core. But the background gamma is slightly high there. Therefore, the sample is placed at the end of the neutron guide system, where the neutron flux is slightly lower in comparison with the location of the instrumental analysis of neutron activation. The detector is placed in a way that the measurement domain is optimum for the half-life. Since after each neutron absorption one or more prompt gamma rays are often emitted, theoretically a counter can measure almost all of the capturing reactions of the neutrons. However, this is not the case in the instrumental method of neutron activation, because in this case, the deployed atoms which are in the capturing period are recorded.

Practically, blue gamma rays' energy is of the order of several mega eV. Most gammas are terminated not at the maximum energy but in the Compton spectrum, and in the prompt gamma neutron activation method, the more energy the gamma ray has, the less chance of absorption of all gamma energy by the detector matter. Therefore, the less energy the gammas have, there is a higher probability of detection at maximum energy of the instrumental method of neutron activation. In figure 1, the change curve of various cases in the application of neutron activation over time are demonstrated. The advantage of using neutron activation in large-sample is that anisotropic samples can be analyzed and there is no need for sampling. On the other hand, problems such as the self-shielding of neutron and weakening of gamma may occur. In the instrumental method of neutron activation with small samples, neutron self-shielding and gamma weakening are negligible, but when larger samples are analyzed, both these factors should be considered.

In the neutron activation through prompt gamma emission from large sample in practical and standard status, we can use the Suki method, in which the operation is performed on a clay pot with the diameter around 15 cm, width of 10 cm, and thickness of 5 cm. The dimensions of the neutron beam are 2 cm3, i.e. smaller than the pot's thickness.

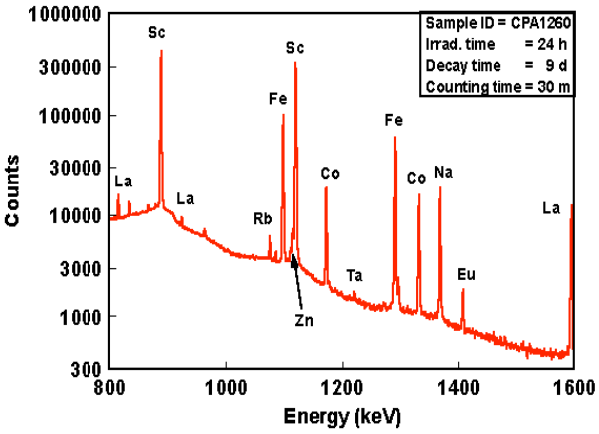

Figure 1. The graph demonstrates the energy for some cases of neutron activation.

The issue of neutron self-shielding and gamma weakening are solved through an internal single-norm method. By this method, the maximum ratio of light levels for gamma detection from sample component (x) and comparator component (y) can be described as follows. To determine the absolute fraction of the components' mass in Suki's clay device, we assume that all the components are oxidized and that the oxides make up the 100% of the sample matter. If all the components can be determined the same as oxides, the assumption can be generally true in the clay device. The internal single-norm method cannot be used as a general method in neutron activation method with prompt gamma from a large sample, since it cannot be assumed

that the components of the sample matter make up a 100%, because all components cannot be determined through the combination of the both methods of PGNAA and NAA, nor can all the components be oxidized. The following equation shows the amount of neutron activation in this method:

$$\frac{Ax}{Ay}=\frac{Nx.bx(Ey.x)\int\int\varphi(En,r)\sigma a,x(En)\varepsilon(E\gamma,x,r)dEndr}{Nx.bx(Ey.x)\int\int\varphi(En,r)\sigma a,y(En)\varepsilon(E\gamma,y,r)dEndr} \quad (1)$$

In the first-order approximation, the equation is simplified by defining $\sigma^1{}_a$ as the microscopic absorption cross-section, and it is expected from this ratio to be the same for any device under radiation. The vector space of the result is $w_x(r)$, which is equal to the normal density distribution. When the result of $\sigma\varphi$ is integrated individually on energy spectrum, equation 2 is yielded. The relative maximum domain of energy, i.e. $\int w_X(r)\in(E_{\gamma,X},r)dr$, should be calculated for each of the sample emission situation according to the incident neutron beams. The $\sigma'_{a,X}\,b_X / \sigma'_{a,y}\,b_y$ ratio should be determined for all the components. In this case, the components' relative matter fraction ($\mathbf{N_x/N_y}$) can be calculated through equation 2.

$$\frac{Ax}{Ay}=\frac{Nx\sigma a,xbx(E\gamma,x)\int wx(r)\varepsilon(E\gamma,x,r)dr}{Ny\sigma a,yby(E\gamma,y)\int wy(r)\varepsilon(E\gamma,y,r)dr} \quad (2)$$

In gamma and neutron transport, we can benefit from Monte-Carlo calculations and Maxwell-Boltzmann velocity method. Various kinds of thermal neutron beams are used in a research. When a beam is formed, we might decide to define the neutron beam cross-section as the uniform level surface, and the source as neutron emitters with a thermal velocity distribution in a specific direction. This approximation saves a lot of time for a complete nuclear reactor modelling which includes moderator and core geometry. In calculation method of thermal neutron beam simulation, we have used Maxwell-Boltzmann velocity distribution function. Neutron-capture rate density in an atom is shown in formula 3:

$$R=\frac{1}{V}\int_0^{¥}(r)\varphi(r,v)\sigma a(v)dvdr \quad (3)$$

In equation 3, if the atom density $\varphi(r)$ is constant and the ratio of volume (V) to neutron flux can be considered linear, the small sample of neutron shielding can be ignored, and we can then use this equation.

Equation 4 calculates the complete thermal flux, and equation 5 can be used to calculate neutron absorption density:

$$< \varphi > th =< \varphi > MB \int_0^{¥} \varphi(v)dv = \int_0^{¥} nvM(v)dv = 2n\sqrt{\frac{2KT}{\pi m}} \quad (4)$$

$$R = \frac{N_0}{V} < \varphi >_{MB} \frac{\sqrt{\pi}}{2}\sqrt{\frac{T_0}{T}}\sigma_{a,0} = \frac{N_0}{V} nv_0\sigma a, 0 \quad (5)$$

If we want to calculate the density of the simulated samples with each other, we can use Monte-Carlo equations.

Simulations have been carried out with the Monte-Carlo MCNP4b instructions. Particles with the volume of 10*0÷*10 mm^2 are used as the counting sides for the interactive neutrons (n.y) in volume elements. This interaction 1/v is counted to determine the neutron density distribution and to compare this with the practical neutron density distribution which is determined by the activity of the copper pieces. Sides' dimensions are chosen to match the pieces of copper wire. Energy distribution used in simulation is Maxwell- Boltzmann velocity distribution in the heat room. These simulated neutrons approximate the sample in a one-dimensional fashion, from a circular design with a diameter of 254 cm which is used as the underlying surface and is directed toward the sample perpendicularly. The neutron beam is simulated uniformly in cross-section. In Monte-Carlo simulation, counting is done between a 0.25 cm transport along y axis from the position where the copper wires are located. This means that counting is performed from 0.5 cm along y axis 250 cm on each side of the copper wire, and the standard deviation in the middle of the sample for the total of 10 sides is equal to 0.3. Through the following equation, we can calculate the length of the wire for neutron density:

$$\chi_r^2 = \frac{1}{D_f}\sum_i \left(\frac{ne,i - \frac{ns,i}{F}}{\sqrt{\sigma_{e,i}^2 + (\frac{\sigma s,i}{F})^2}} \right)^2 \quad (6)$$

The chi-square is the reduced χ_r^2, the degrees of differentiation D_f, neutron density $n(m^{-3})$, coupling coefficient of equation F, neutron density standard deviation $\sigma(m^{-3})$, e index for the operator, s index for the simulator, and i for the pure copper wire.

$$F = \frac{\sum_i n_{e,i}}{\sum_i n_{s,i}} \quad (6\text{-}1)$$

$$\sigma F = F\sqrt{(\frac{\sqrt{\sum_1 (\sigma e,i)^2}}{\sum_1 ne,i})^2 + \sqrt{(\frac{\sqrt{\sum_1 (\sigma s,i)^2}}{\sum_1 ns,i})^2 \sqrt{\chi^2 r}}} \quad (7)$$

In equation 7, σF can be calculated.

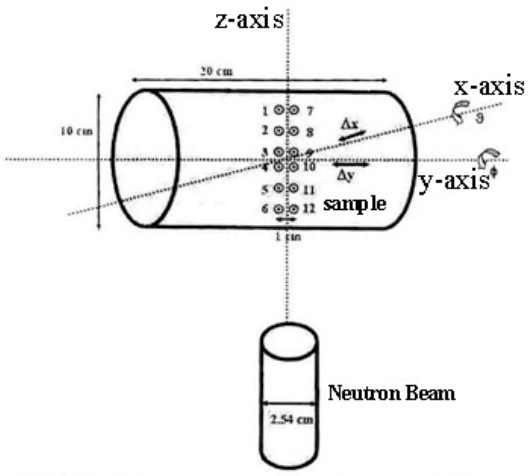

Figure 2. Neutron Beam Schematic in Pure Copper Wire.

In figure 2, a schematic view of the neutron beam in copper wire sample has been demonstrated. Rotation around its axes has also been illustrated. The aim of this experimental method is to compare the neutron density distribution yielded from experiments $(n_e(r))$ and the simulated amount $(n_e(r))$. For the comparison, which is made with a measured piece of copper in neutron relative density experiment, simulation of the mean value $(n_e(r))$ is used in the positions near a piece of copper. The reduction comparison in $(\chi r^2)\lambda^2$ facilitates the reverse degree of the stable balance between the experiment and the simulation. Sometimes we are faced with this problem that in the simulation no neutron is counted in one of the corresponding sides with the copper piece. In this case, uncertainty in MCNP is equal to zero, which occurs in less than %0.0001 of the cases. To make sure that all these sides have a correct uncertainty, uncertainty of these sides is considered equal to the uncertainty that is resulted when a neutron is counted instead of zero. Since $n_{s,i}$ and $n_{e,i}$ might be deviated due to the erroneous estimation of the detector's impact, F is used for the coupling of these distributions. It is supposed that exposure and measurement are equal for all samples. In calculating the amount of F in the sample containing sand and the sample containing graphite and lithium sulfate in simulation, neutrons are counted in all directions. This condition does not exist for the air sample based on an amount of F with a standard deviation larger than (σ_F). Since F should be equal for all the samples under the same exposure conditions for determining the activity, the amounts for samples containing sand and samples containing graphite and lithium sulfate should be added to the sample containing air. Table 1 includes the amounts coupling factor, transports, and rotations in relation with the standard deviation and the error changes resulting from matching.

Table 1. In terms of the standard deviation and the amount of rotation and the error to the due

sample matter / parameter	sand	air	mixture
without correction for Δx,Δy, ϑ, φ			
χ^2	48	102	83
with correction for Δx,Δy, ϑ, φ			
χ^2	33	58	49
F	1.420±0.010	1.43	1.437±0.007
Δy (mm)	0.005±0.018	-0.6183±0.0004	0.499±0.002
Δx (mm)	-0.3831±0.0011	-1.3320±0.0006	0.4990±0.0009
ϑ (°)	-0.23±0.03	2.2196±0.0023	1.1413±0.0023
φ (°)	0.264±0.017	1.3407±0.0017	1.160±0.003

For achieving better matching between the results of the experiments and the simulations, it is necessary to calculate the error related to imprecision in determining the position of the PTFE preservative in relation to the neutron beams. The center of mass for each PTFE sheath in the experiment in the most ideal condition possible is placed in relation to the center of the neutron beam, with the copper wires perpendicular to the neutron beams direction. Therefore, it is allowed for the manual positioning in which the sample small deviations along y-axis (Δy) and x-axis equivalent to rotations around Y (Φ) and axis θ. By using equation 7, we can calculate neutron activation method around the axes. In the process of comparing, a minimum amount x_r^2 with a network of variables is defined: for all the parameters $\theta, \varphi, \Delta x, \Delta y, F$, minimum amount x_r^2 is defined by using non-linear least squares method. For the amount of F, in the comparing process with the use of air containing sample, there is not much room for maneuver. In the next part, the difference between $n_s(r), n_e(r)$ as a fraction of neutron density distribution in a position of the sample will be mentioned, where neutron beam enters $(n(r_{in}))$. This shows a more tangible impact than imprecision in simulation according to the rate experiment $n_e(r)$especially farther from neutron beams where amount of $n_e(r)$and $n_e(r)$ are infinitesimal. In both of the researches carried out in this chapter between experiments and simulations, considering the neutron density distribution in a large sample under radiation with a thermal neutron beam with a diameter of 2.54 cm, a good equivalence has been obtained. Firstly, neutron density distribution with %2 $n_e(r_{in})$ is in equilibrium for all samples. Secondly, F is in stable equilibrium for both of the determined amounts. If we want to achieve the average distance between the atomic mass and d direction, we have:

$$dCM = \frac{\sum_{1} nad}{\sum_{V} na} \tag{8}$$

$$\Delta d = \frac{\sum_{V} na\left|d - dCM\right|}{\sum_{V} na} \tag{9}$$

The amount of d center of mass (d_{cm}) is calculated in equation 8, and the average distance between neutron and center of mass in the direction of $(\Delta d)d$ is resulted from equation 9. The amount of Δr can be achieved by substituting r and d.

$$P(\sum s, \sum t) = d + \left[f(\sum s, \sum t)^{1-h(\sum s, \sum t)} + \exp\left(-\left(\ln \frac{(\sum s)}{1cm^{-1}} - g(\sum s, \sum t) \right) \right) \right]^{\frac{1}{1-h(\sum s, \sum t)}} \tag{10}$$

In equation 10, four functions (h.d.f.g) have been used. For correction the unit problem, in the natural logarithm of -1, 1 cm is inserted. The d function in the minimum $\sum_s$ is the horizontal asymptote which shows the probability of neutron absorption from the incident beam or scattered neutron by the PTFE bottle. This probability is larger than the probability of neutron absorption asymptote in copper slug places at 180 degree angle, because PTFE weakens the neutron beam. The f function demonstrates the probability of scattered neutron absorption with the sample matter when $\sum_s$ is infinite. All function except d are dependent on the sample matter. Functions g and h are in linear proportion with the ratio $\sum_s / \sum_t$. By changing the functions in equation 10, it is observed that the first part (d) demonstrates a weakening in the shell. The second part shows the probability of scattered neutron absorption in the sample matter or the shell. When scattering is infinite, the third part defines the neutron relative density curve, which is measured outside the sample, based on the scattering in the sample matter or the shell.

3. CONCLUSION

In the mentioned cases of laboratory research, neutron density distribution is performed in a large sample under radiation to a thermal neutron beam with a definite diameter according to a good procedure. The obtained sample has a stable equilibrium. This sample is equal to the ratio $\sum_s / \sum_t$ and transport coefficient, but the effective atomic mass, except for the number of all absorbed neutrons in the sample matter and the center of mass for neutron density distribution, is practically equal. If a change occurs in the distance, it is dependent on the amount of atomic mass. When neutron density distribution in the simulated matter is performed with absorption

cross-section and macroscopic scattering, the resulted errors in the number of neutrons absorbed and the assumed position of center of mass ($\Delta d, \Delta r$) are all dependent on the effective atomic mass.

In conclusion, in the experiment, no correction should be applied to the effective atomic mass in the sample matter in neutron activation method based on large sample emitted prompt gamma. The free gas method can be used from the methodology with the help of M_e equal to 1000 for the simulated sample matters. Also, in LS-PGNAA, no range is directly calculated, expect for the ratio Ω_x / Ω_{ref} for calculating gamma weakening factor and neutron self-shielding. Therefore, no equivalence is necessary between the measurement range and the calculated effective spatial angle.

To analyze the components of the sample matter with an effect line distribution of the heterogeneous component, only the methodology should be compatible. When the spectrum of the activation method based on neutron from prompt gamma from this sample should be constant, the sample might move like a screw with both rotation and transport. The advantage of the rotation method is that neutron density distribution in the sample matter is more homogenous than the time when the sample does not rotate. In the existing state in gamma activation method based on prompt gamma emission in large sample, neutron density distribution is more homogenous when the sample matter is radiated with a synchronic exposure.

REFERENCES

[1] Alfassi, Z.B. , Chung, C.Prompt gama neutron activation analysis, CRC Press, Boca Raton, Florida, USA (1995)

[2] Lin, X. , henkelmann, R. , Instrumental neutron activation analysis of large samles: A poilt experiment, J. Radioanal. Nucl. Chern. 251, 197-204(2002)

[3] Overwater, R. M.W. , Hoogenboom, J. E. , Accounting for the thermal flux depression in Voluminous sample for the instrumental neutron activation analysis, Nucl. Sci. Eng. 117,141-157 (1994)

[4] Oura, Y. , Ebihara, M. , Yoneda, S. , Nakamura, N. , Chemical composition of the kobe Meteorite; Neutron-induced prompt gamma ray analysis study, Geochem. J.36,295-307(2002)

[5] Briesmeister, J. , MCNP – a general Monte Carlo N-partical transport code, version 4B Los Alamos national laboratory, Los Alamos, USA (1997)

[6] Mackey, E. A. , Personal Communication, (1998)

[7] Lindstrom, R. M. , Firestone, R. B. , Paviotti-Corcuera, R. , Summary report of the third research .Coordination meeting Development of a database for prompt gamma-ray neutron activation analysis. , International nuclear data committee, IAEA, Vienna, Austria(2003)